

EFFECT OF PIGMENTS ON BOND STRENGTH BETWEEN COLOURED CONCRETE AND STEEL REINFORCEMENT

JOSEPH J. ASSAAD*, MATTHEW MATTA, JAD SAADE

University of Balamand, Department of Civil and Environmental Engineering, Balamand, PO Box 100, Al Kourah, Lebanon

* corresponding author: joseph.assaad@balamand.edu.lb

ABSTRACT. The effect of pigments on mechanical properties of coloured concrete intended for structural applications, including the bond stress-slip behaviour to embedded steel bars, is not well understood. Series of concrete mixtures containing different types and concentrations of iron oxide (red and grey colour), carbon black, and titanium dioxide (TiO_2) pigments are investigated in this study. Regardless of the colour, mixtures incorporating increased pigment additions exhibited higher compressive and splitting tensile strengths. This was attributed to the micro-filler effect that enhances the packing density of the cementitious matrix and leads to a denser microstructure. Also, the bond to steel bars increased with the pigment additions, revealing their beneficial role for improving the development of bond stresses in reinforced concrete members. The highest increase in bond strength was recorded for mixtures containing TiO_2 , which was ascribed to formation of nucleus sites that promote hydration reactions and strengthen the interfacial concrete-steel transition zone. The experimental data were compared to design bond strengths proposed by ACI 318-19, European Code EC2, and CEB-FIP Model Code.

KEYWORDS: Coloured concrete, iron oxide pigment, carbon black, titanium dioxide, durability, bond strength.

1. INTRODUCTION

Pigments including iron oxide (IO), carbon black (CB), and titanium dioxide (TiO_2) are finely ground particles for integral colouring of concrete and cementitious materials intended for architectural applications [1–3]. Often manufactured as per ASTM C979 [3] specification, the pigments are bound onto the surface of cement grains, thus altering the colour characteristics by absorbing certain wavelengths of the visible light and reflecting others. The IOs are synthetic colourants manufactured to display a variety of colours (i.e., red, grey, yellow, etc.), thus infusing the concrete with their shades [4, 5]. These pigments are stable in the high-alkaline Portland cement environment, conferring proper colour fastness to sunlight exposure and resistance to weathering effects. The CB is an economical black colourant with high tinting strength produced from petroleum and charring organic materials [1, 6]. Compared to IO, the CB generally disrupts the air-entrainment and increases the vulnerability of concrete to leaching when exposed to repeated wet/dry cycles [6]. The white-coloured TiO_2 mostly occurs in the natural rutile and anatase crystal forms [7, 8]; it is normally used with white cement and other pozzolanic materials (metakaolin) to brighten the cementitious mixture.

Earlier studies showed that the pigment characteristics (i.e., type, fineness, mineralogy, morphology, solubility, etc.), additions rates, and dispersion can drastically alter the fresh and hardened concrete properties [9–11]. For instance, it is accepted that pig-

ments absorb part of the free mixing water because of a significantly higher surface area (vs. cement), thus requiring increased water demand and/or high-range water reducer (HRWR) to achieve a given workability [12–14]. Meng et al. [15] reported that the drop in fluidity due to TiO_2 can be controlled through HRWR and slag additions. If poorly dispersed, added pigments may agglomerate in the cement matrix, causing unreacted pockets or weak zones that decrease mechanical properties [15, 16]. Lopez et al. [17] suggested using the mortar phase, while others recommended the use of extended mixing time [18] or water-based colourants [19] to improve pigment dispersibility.

Despite their chemically inert nature, most studies showed that synthetic IO and CB pigments lead to increased strength and durability of cementitious materials. This is generally associated to a micro-filler effect that blocks the capillary pores and leads to a denser microstructure [9, 20, 21]. Yildizel et al. [22] found that yellow and black IOs lead to increased strength and resistance to water permeability. Mortars produced using red pigments exhibited relatively higher pore ratios, which detrimentally affected freeze/thaw resistance and durability. Assaad et al. [11] reported that strength and bond to existing substrates increased when red or yellow pigments are incorporated by up to 6% of cement mass. The curtail in strength at high pigment rates (above 6%) was related to improper hydration reactions resulting from the excessive amount of powders that are adsorbed onto the cement grains. Masadeh [23] found that

Physical properties	Specific gravity	Median particle size	Soundness	Blaine fineness	Lightness (L -value)
	3.15	26.5 μm	0.04 %	3150 cm^2/g	88.5
Chemical properties	CaO	SiO ₂	Al ₂ O ₃	Fe ₂ O ₃	MgO
	68.5 %	21.8 %	4.15 %	0.27 %	1.18 %

TABLE 1. Physical and chemical properties of white cement.

CB incorporated up to 0.5 % of cement mass reduces the concrete chloride permeability and corrosion rates of inserted steel bars. Inoue et al. [24] noted that the CB treatment using aqueous solution of humic acids helps improving the dispersibility together with a reduced interaction with air-entraining surfactants and superior adhesion to the cement matrix (i.e., less leaching).

In addition to the micro-filler effect, numerous researchers found that TiO₂ can participate in the cement hydration process, at least as nucleation sites, to accelerate setting times and promote strength development [15, 16, 25, 26]. Chen et al. [27] showed that concrete durability and resistance to water infiltration significantly improved with 3 % TiO₂ additions, given the conversion of greater volume of calcium hydroxide (CH) crystals into C-S-H gels. Zhang et al. [28] reported that TiO₂ acts as a filler in empty spaces and crystallization centre of CH to refine the concrete microstructure including its resistance to chloride ion penetration. Folli et al. [29] speculated that the strength improvement might be related to alteration in packing density and nucleus orientation around the interfacial transition zones, rather than increased amounts of hydration products.

2. CONTEXT AND PAPER OBJECTIVES

The performance of coloured concrete in structural members, including the extent to which the use of pigments would alter the bond strengths to embedded steel bars, is not well understood. Generally, the transfer of stresses between the reinforcement and surrounding concrete is attributed to chemical adhesion and mechanical bearing arising from the concrete surface around the steel ribs [30, 31]. The parameters affecting the bond are broadly related to the reinforcement characteristics (i.e., yield strength of bar, size, geometry, epoxy coating, cover, position in cast member, etc.) and concrete constituents and properties (i.e., density, strength, workability, presence of fibres, mineral admixtures, etc.) [32]. The spliced or developed lengths are computed by relevant models proposed by various building codes; for example, ACI 318-19 [33] considers that the development length for deformed bars in tension members is inversely proportional to the square root of compressive strength, multiplied by specific factors to account for special considerations due to the reinforcement size, lightweight concrete, top bars, epoxy-coated bars, and contribution of confining

transverse reinforcement. Yet, limited attempts have been made to assess the validity of existing models and design provisions in the case of coloured concrete.

This paper is a part of a comprehensive research project undertaken to assess the effect of pigments on durability and mechanical properties of coloured concrete mixtures. Two concrete series made with 350 and 450 kg/m^3 cement content and various concentrations of IO (red or grey colour), CB, and TiO₂ pigments are investigated. Tested properties included the compressive strength, splitting tensile strength, modulus of elasticity, and bond stress-slip behaviour to reinforcing steel bars. The experimental data were compared to design bond strengths proposed by relevant building codes including ACI 318-19 [33], European Code EC2 [34], and CEB-FIP Model Code [35]. Data reported herein can be of interest to civil engineers and architects seeking the use of pigments in coloured concrete intended for structural applications.

3. EXPERIMENTAL PROGRAM

3.1. MATERIALS

White-coloured Portland cement conforming to ASTM C150 Type I was used in this study. Its physical and chemical properties are listed in Table 1.

The gradations of siliceous sand and crushed limestone aggregate were within the ASTM C33 specifications. The specific gravity for the sand, fineness modulus, and absorption rate were 2.65, 3.1, and 0.75 %, respectively. Those values were 2.72, 6.4, and 1 %, respectively, for the coarse aggregate, while the nominal maximum particle size was 20 mm. Naphthalene-based HRWR was used; its specific gravity, solid content, and maximum dosage rate were 1.2, 40.5 %, and 3.5 % of cement mass, respectively.

Commercially available IO (i.e., red and grey colour), CB, and TiO₂ pigments were used. As shown in Figure 1, the red and grey coloured IOs had almost spherical shapes; their specific gravities were 4.64 and 4.8, respectively, while their Fe₂O₃ contents were 97.5 % and 98.8 %, respectively. The white-coloured TiO₂ is rutile-based manufactured by the chloride process; it also possesses round shape (Figure 1) with a specific gravity of 4.1. The CB is produced by combustion of aromatic petroleum oil feedstock and consists essentially of pure carbon (i.e., > 98 %); its specific gravity was 2.05.

The particle size gradation curves obtained by laser diffraction for the various pigments are plotted in

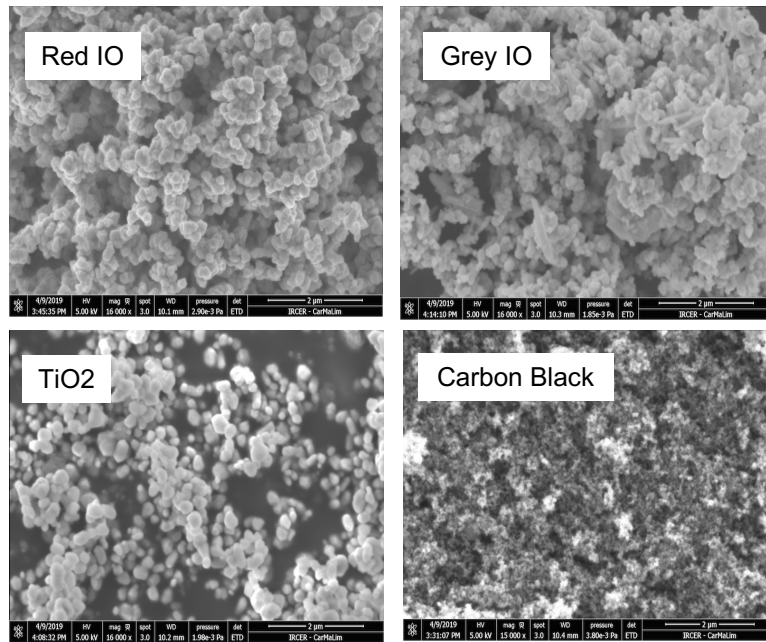


FIGURE 1. Morphology of various pigments used.

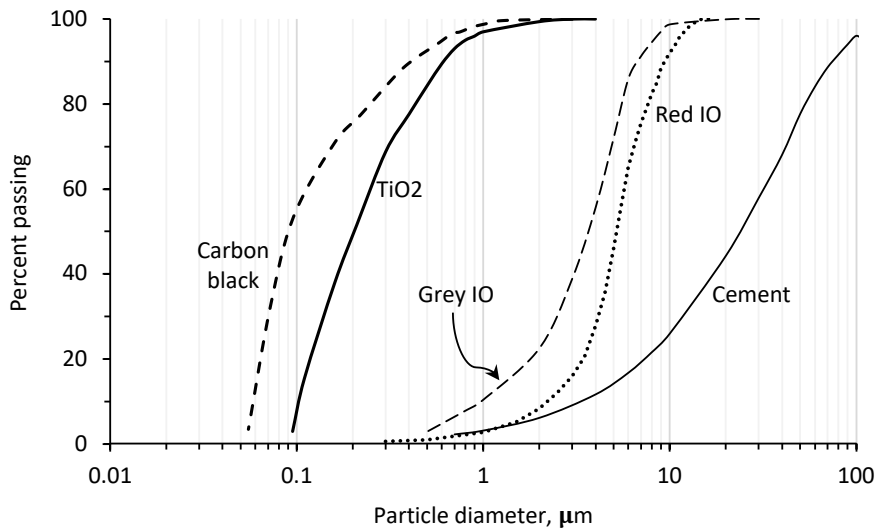


FIGURE 2. Particle size distribution curves for the cement and various pigments.

Figure 2. Generally speaking, the fineness of IO pigments is pretty close to each other; the median diameter (d_{50}) computed as the size for which 50% of the material is finer for the grey and red IO is 4.1 and 5.3 μm , respectively. The TiO_2 and CB were remarkably finer, which shifted the gradation curves towards much smaller particle sizes. The resulting d_{50} dropped to 0.21 and 0.092 μm for the TiO_2 and CB, respectively.

Deformed steel bars complying to ASTM A615 No. 13 were used in this work to evaluate the effect of pigments on bond stress-slip properties of coloured concrete to embedded rebars. The bar nominal diameter (d_b), Young’s modulus, and yield strength (f_y) were 12 mm, 205 GPa, and 520 MPa, respectively.

3.2. MIXTURE PROPORTIONS

Two control concrete mixtures containing 350 (or, 450) kg/m^3 cement with 0.5 (or, 0.42) water-to-cement ratio (w/c) were considered; the corresponding 28-days $f'c$ was 26.7 and 34.2 MPa, respectively. The fine and coarse aggregate contents in the lean concrete mixture were 830 and 1020 kg/m^3 , respectively; while these were 790 and 925 kg/m^3 in the higher strength concrete mix. The resulting sand-to-total aggregate ratio was 0.45. The HRWR dosage was either 2.6% or 2.35% of cement mass, respectively, in order to secure a fixed workability corresponding to a slump of 210 ± 10 mm.

The IO, CB, and TiO_2 pigments were incorporated at three different concentrations varying from 1.5% to 4.5% of cement mass, at 1.5% increment rates. The

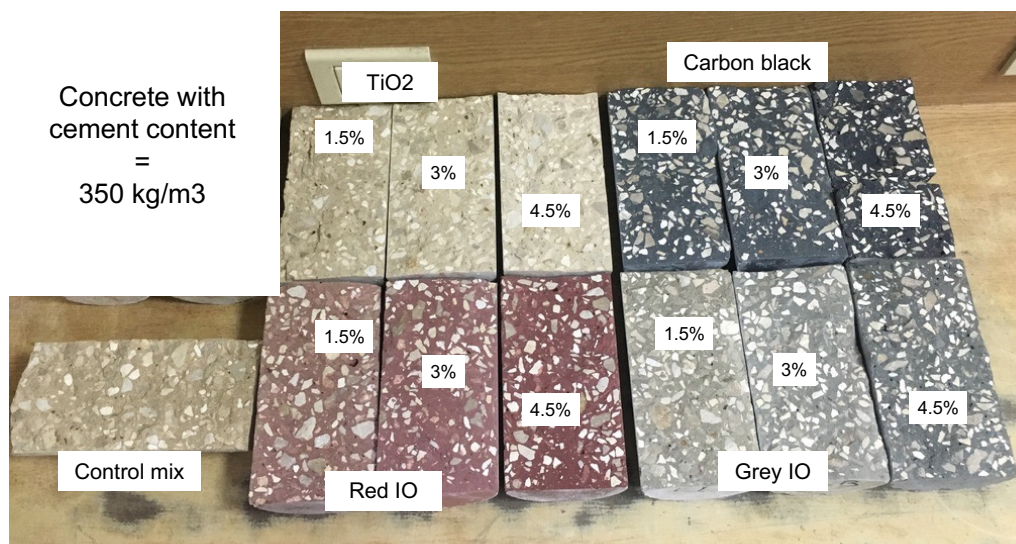


FIGURE 3. Photo of coloured cylinders after the splitting tensile test.

mixing sequence consisted on homogenizing the fine aggregate, coarse aggregate, and powder pigment for 3 minutes to ensure efficient dispersion of colourant materials. The cement, water, and HRWR were then sequentially introduced over 2 minutes. After 30 sec rest period, the mixing resumed for 2 more minutes. The ambient temperature and relative humidity (RH) remained within $23 \pm 3^\circ\text{C}$ and $55 \pm 5\%$, respectively.

3.3. TESTING PROCEDURES

3.3.1. FRESH AND HARDENED PROPERTIES

Right after mixing, the workability and air content were determined as per ASTM C143 and C231, respectively. The concrete was cast in 100×200 mm cylinders to determine the density, compressive strength (f'_c), and splitting tensile strength (ft) as per ASTM C642, C39, and C496, respectively [36–38]. All specimens were demoulded after 24 hours, cured in water, and tested after 28 days. Averages of 3 values were considered. The modulus of elasticity (E) was determined through ultrasonic pulse velocity (UPV) measurements using 100×200 mm concrete cylinders, as per ASTM C597 [39]. The pulse velocity was computed as the ratio between the 200 mm length of the concrete specimen to the measured transit time. The E was computed using the conventional wave propagation equation in solid rocks, expressed as: $E, GPa = [(\rho \times UPV^2)/g] 10^{-2}$, where g is gravity acceleration (9.81 m/s^2) and ρ is the concrete density (kg/m^3) [1, 31].

3.3.2. COLOURIMETRY

The L , a , and b colour coordinates were determined following the Commission Internationale d'Eclairage (CIE) system using a portable colourimeter. The L -value reflects the colour lightness varying from 0 (black) to +100 (white), a -value represents the chromatic intense of magenta/red (+127) and green (–128), and b -value the chromatic intense of yellow (+127) and

blue (–128) [19, 40]. The specimens were oven-dried for one day at $50 \pm 5^\circ\text{C}$ prior to testing. The measurements were realized using the broken cylinders after the tensile splitting test, as shown in Figure 3. Special care was taken to position the colourimeter sensor in the mortar phase (not the aggregate particle); while an average of 6 measurements was considered. The colour deviation ($\Delta(E)$) due to pigment additions from the control mix was determined as:

$$\Delta(E) = \sqrt{(L_C - L)^2 + (a_C - a)^2 + (b_C - b)^2},$$

where $L_C = L_{Control}$, $a_C = a_{Control}$, $b_C = b_{Control}$.

3.3.3. BOND TO STEEL REINFORCEMENT

The direct bond method was used to determine the bond stress-slip properties of concrete mixtures, in accordance with RILEM/CEB/FIB specification [41]. The bars were vertically centred in the 150 mm cubic moulds (Figure 4); the embedded length was 60 mm ($5 d_b$) and PVC bond breaker was inserted around the bar at the concrete surface to reduce the concentration of stresses during loading. After 24 hours from casting, the specimens were demoulded and covered with plastic bags to cure at $23 \pm 3^\circ\text{C}$ for 28 days. The direct bond test was realized using a universal testing machine, whereby the pullout load and slips of the steel bar relative to the concrete block are recorded [30, 42]. The tensile load was gradually applied until failure at a rate hovering 0.25 kN/sec .

4. TEST RESULTS AND DISCUSSION

4.1. HRWR DEMAND

Table 2 summarizes the HRWR demand and colour coordinates for mixtures prepared with various pigment types and concentrations. In line with current literature [1, 4, 8], the demand for HRWR increased with pigment additions, given their higher fineness

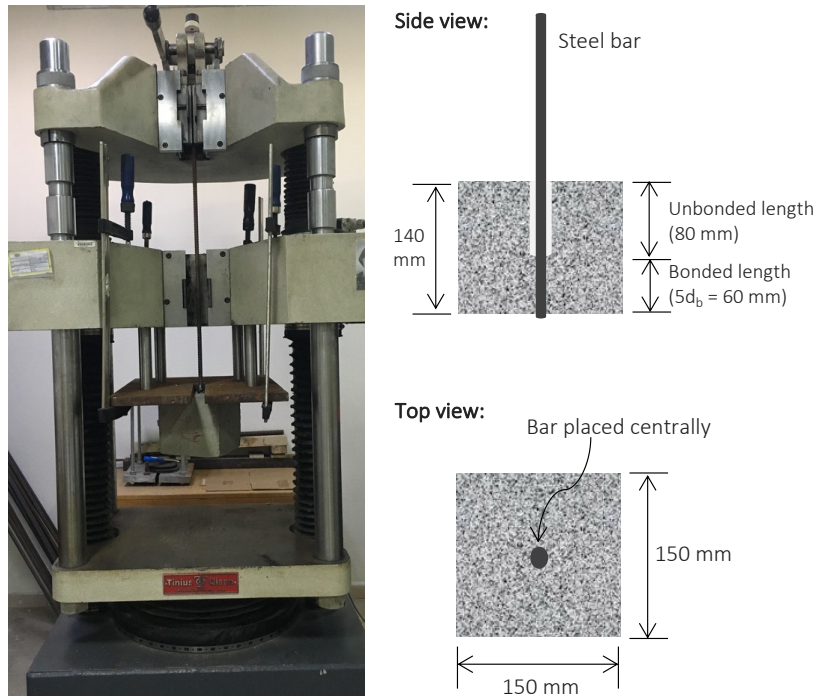


FIGURE 4. Photo of the experimental testing of bond stress-slip properties.

Mixture codification	HRWR [% of cement]	Slump [mm]	Air content [%]	Density [kg/m] ³	<i>L</i>	<i>a</i>	<i>b</i>	$\Delta(E)$
350-Control	2.6	205	2.8	2320	67.8	5.6	19.3	–
350-Red-1.5 %	2.6	205	n/a	2315	55.2	12.8	12.9	15.8
350-Red-3 %	2.9	200	2.7	2330	51.9	16.1	10.6	21.0
350-Red-4.5 %	3.2	200	2.9	2375	44.4	19.8	12	28.3
350-Grey-1.5 %	2.7	195	n/a	2330	61.9	2.2	12.4	9.6
350-Grey-3 %	2.9	205	3.1	2360	58.4	0.8	7.2	16.0
350-Grey-4.5 %	3.1	205	n/a	2350	49.4	-0.1	4.0	24.6
350-TiO2-1.5 %	2.7	210	n/a	2310	72.0	5.3	19.8	4.3
350-TiO2-3 %	3.0	210	3	2340	71.9	5.4	19.7	4.2
350-TiO2-4.5 %	3.1	195	2.9	2380	76.3	4.4	17.9	8.7
350-CBlack-1.5 %	2.9	190	n/a	2350	42.4	-0.2	-0.2	32.5
350-CBlack-3 %	3.5	195	3.2	2340	42.2	-0.5	-0.7	33.0
350-CBlack-4.5 %	3.6	205	3.4	2390	31.0	-0.05	-1.2	42.4
450-Control	2.4	205	3	2345	68.3	5.7	19.1	–
450-Red-3 %	2.5	210	3.1	2385	48.8	19.0	10.8	25.0
450-Grey-3 %	2.8	200	3	2385	56.2	0.58	6.9	17.9
450-TiO2-3 %	2.7	200	2.8	2405	77.1	5.1	19.1	8.9
450-CBlack-3 %	3.2	205	3.5	2415	41.9	-0.4	-0.8	33.6

The mix codification refers to cement content-Pigment type-Pigment dosage.
n/a refers to not tested.

TABLE 2. Effect of pigment types and concentrations on workability and colourimetry properties.

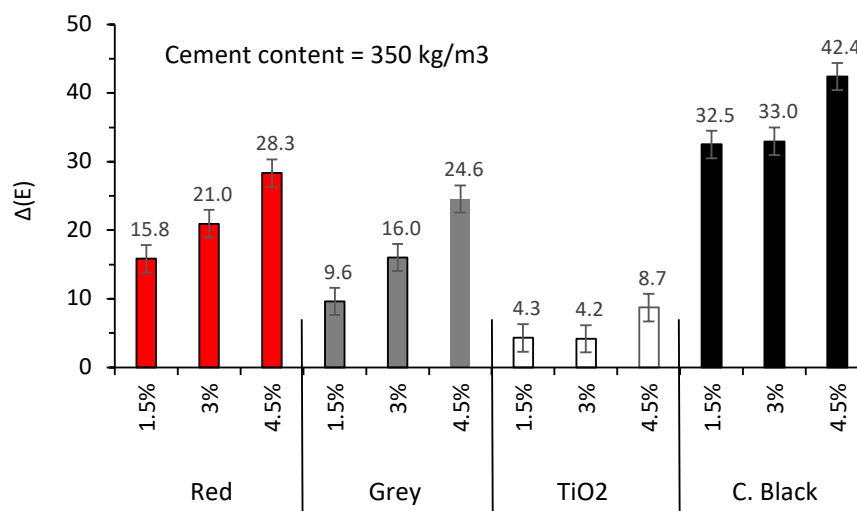


FIGURE 5. Effect of pigment type and concentration on $\Delta(E)$ variations for concrete prepared with 350 kg/m³ cement.

that absorbs part of the mixing water and results in requirement of additional superplasticizing molecules to ensure the targeted slump of 210 ± 10 mm. For example, at a 3% pigment rate, the HRWR dosage varied from 2.6% for the 350-Control mix to 2.9% and 2.85% for the 350-Red-3% and 350-Grey-3% mixtures, respectively. The increase in HRWR was particularly pronounced for the CB pigment, given its extremely fine particles [13]. Hence, the HRWR reached 3.45% and 3.6% for the concrete containing 3% or 4.5% CB, respectively.

4.2. COLOURIMETRY

As can be noticed in Table 2, the lightness of colour (L -value) increased from 67.75 for the 350-Control mix to 72 and 76.3 with the addition of 1.5% and 4.5% TiO₂, respectively, which can be attributed to the intrinsic white-coloured nature of this pigment [26, 29]. Yet, as expected, the L -value followed a decreasing trend when darker pigments were used; it dropped to 49.35, 44.35, and 31 for mixtures containing 4.5% grey, red, and CB pigments, respectively. To the other end, the magenta chromatic intense (i.e., a -value) varied from 5.55 to 16.1 for the 350-Control and 350-Red-3% mixtures, respectively, while in contrast, the highest b -value of 19.75 corresponded to the 350-TiO₂-1.5% mix. Concrete mixtures prepared with CB exhibited negative a and b values, reflecting the black colouring effects of such powders.

As shown in Figure 5, the mixtures containing the white-coloured TiO₂ pigments exhibited the lowest $\Delta(E)$ values, reflecting relatively limited variations with respect to the control mix. The incorporation of red or grey IO pigments gradually increased the $\Delta(E)$ values that varied from 9.6 to 28.3, while the CB-modified mixtures exhibited the highest $\Delta(E)$ that varied from 32.5 to 42.4. It should be noted that $\Delta(E)$ steadily increased with pigment additions (Figure 5), without showing a clear stabilization tendency that

reflects colour saturation [11, 17]. This can be attributed to the relatively reduced cement volume (i.e., about 11% of the overall concrete mix), thus requiring additional pigment powders to achieve colour saturation. Additionally, the beige-like colour of natural sand could have affected the pigment tinting strength, which reduced the tendency towards the colour saturation [10, 11].

4.3. HARDENED PROPERTIES

The effect of pigment type and concentration on the 28-days $f'c$ for concrete prepared with 350 kg/m³ cement are summarized in Table 3, and plotted in Figure 6. Regardless of the colour, mixtures incorporating increased pigment additions exhibited higher strength values. For example, compared to the 26.7 MPa value obtained for the control mix, the $f'c$ increased to 29.7 and 34.9 MPa for the mixtures containing 1.5% and 4.5% red IO, respectively. Such values reached 30 and 34.2 MPa for the mixtures containing 1.5% and 4.5% grey IO, respectively. This could be associated to the micro-filler effect and enhanced packing density that lead to a denser microstructure capable of supporting higher loads. Yildizel et al. [22] reported that IO pigments are inert materials (i.e., do not react with water) that fill the interspaces and capillary pores in cementitious systems, leading to an improved resistance against permeability and attack of aggressive ions.

For the given concentration, the effect of CB on strength development is pretty similar or slightly higher than the IO pigments. Hence, the $f'c$ reached 35.1 MPa for the 350-CBlack-4.5% mixture. Knowing the inert nature of such powders, the increase in strength can be physically related to the micro-filler effect that enhances packing density of the cementitious matrix.

The highest increase in $f'c$ was recorded for concrete mixtures prepared with TiO₂ additions; this

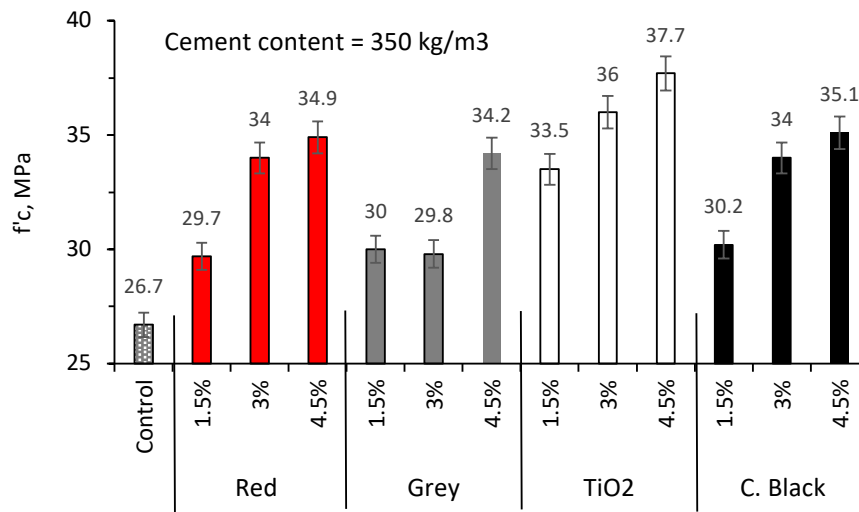


FIGURE 6. Effect of pigment types and concentrations on hardened properties and bond to steel bars.

Mixture codification	7-d $f'c$ [MPa]	28-d $f'c$ [MPa]	ft [MPa]	UPV [km/s]	E [GPa]	τ_u [MPa]	δ_u [mm]
350-Control	14.8	26.7	2.16	3.55	29.8	11.36	4.1
350-Red-1.5 %	17	29.7	2.28	3.58	30.2	11.94	5.3
350-Red-3 %	20.1	34	2.41	3.6	30.8	18.00	10.3
350-Red-4.5 %	19.8	34.9	3.06	3.62	31.7	17.78	10.5
350-Grey-1.5 %	17.2	30	n/a	3.5	29.1	n/a	n/a
350-Grey-3 %	20.2	29.8	2.86	3.62	31.5	12.74	4.9
350-Grey-4.5 %	20.6	34.2	3.36	3.58	30.7	14.05	6.1
350-TiO2-1.5 %	19.7	33.5	2.62	3.57	30.0	17.25	6.2
350-TiO2-3 %	19.6	36	2.7	3.66	32.0	n/a	n/a
350-TiO2-4.5 %	20.6	37.7	3.22	3.62	31.8	20.70	7.8
350-CBlack-1.5 %	19	30.2	2.87	3.6	31.0	15.34	4.4
350-CBlack-3 %	18.8	34	n/a	3.72	33.0	n/a	n/a
350-CBlack-4.5 %	20.5	35.1	3.28	3.8	35.2	17.89	5
450-Control	23.4	34.2	2.56	3.7	32.7	18.90	5.8
450-Red-3 %	27.3	38.9	3.76	3.8	35.1	23.41	11.5
450-Grey-3 %	25.8	42.3	n/a	3.83	35.7	19.78	6.3
450-TiO2-3 %	28.6	44.5	3.94	3.7	33.6	24.85	9.2
450-CBlack-3 %	27.6	41.6	3.85	3.9	37.4	21.96	7.2

n/a refers to not tested.

TABLE 3. Effect of pigment types and concentrations on workability and colourimetry properties.

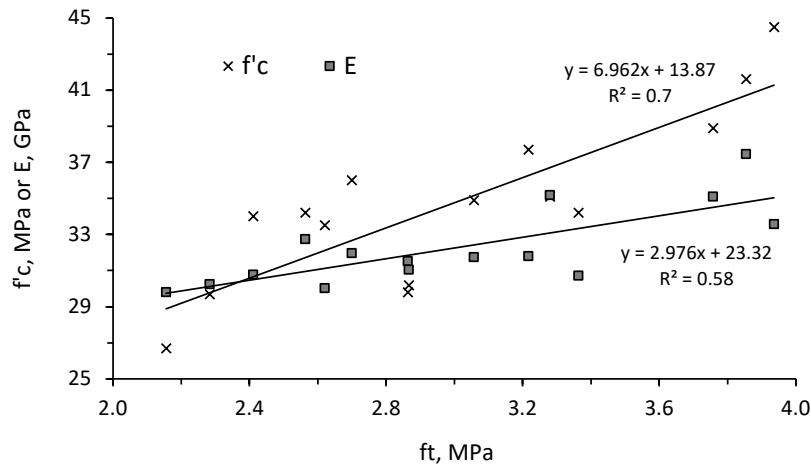


FIGURE 7. Relationships between f_t with respect to f'_c and E responses for all tested concrete mixtures.

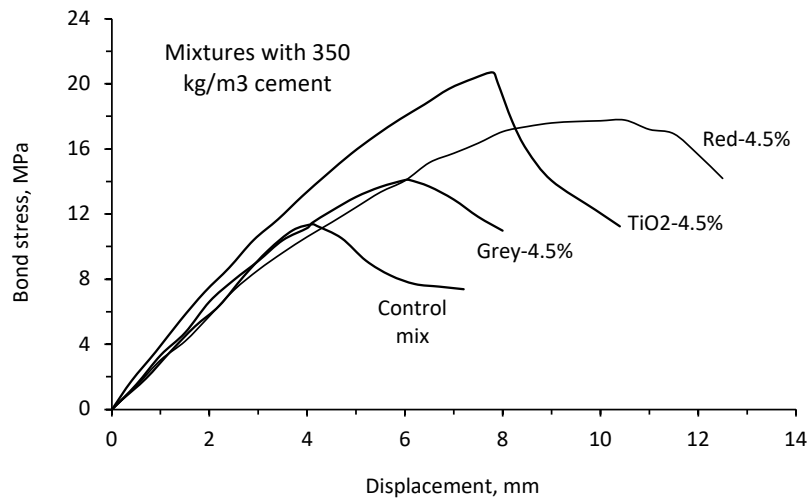


FIGURE 8. Typical bond stress vs. displacement curves for mixtures prepared with 350 kg/m^3 cement.

reached 33.5 and 37.7 MPa at 1.5% and 4.5% rates, respectively. Besides the micro-filler effect, the increase in strength may be ascribed to the formation of nucleation sites that promote hydration reactions and precipitate additional gels in the hardened matrix [16, 29]. The hydration products grow around the TiO_2 particles, causing the formation of secondary C-S-H in the capillary pores that reduces the porosity of the matrix. As shown in Table 3, the f'_c significantly increased from 34.2 MPa for the 450-Control mix to 44.5 MPa for the 450- TiO_2 -3% concrete, which can be associated to the micro-filler effect prompted with additional C-S-H hydrating compounds that could refine the concrete microstructure [27, 28].

The effect of pigment type and concentration on f_t and E properties is quite similar to the one observed on f'_c responses. Hence, the strength increased with IO and CB pigments, while being particularly pronounced with the use of TiO_2 (Table 3). Moderate relationships with correlation coefficients (R^2) larger than 0.58 are obtained between the hardened prop-

erties for all tested concrete mixtures prepared with 350 and 450 kg/m^3 cement, as shown in Figure 7.

4.4. BOND STRESS-SLIP BEHAVIOR

Table 3 summarizes the ultimate bond strength (τ_u) at failure and corresponding slip (δ_u) for all tested concrete mixtures. It is worth noting that the coefficient of variation (COV) for τ_u responses determined for selected mixtures varied from 9.6% to 14.7%, representing an acceptable repeatability. The steel bars did not reach their yielding state during pullout testing (i.e., the yielding load is 58.8 kN). A pullout mode of failure occurred for all tests, whereby the concrete crushed and sheared along the embedded steel region with no visible cracks on the external concrete specimens [30, 31].

Typical bond stress-slip (τ vs. δ) curves determined for the 350-Control mix and those incorporating different pigment types and concentrations are plotted in Figure 8. All curves are initially linear, which can be ascribed to the adhesive component of the bond and mechanical interlock that takes place between the

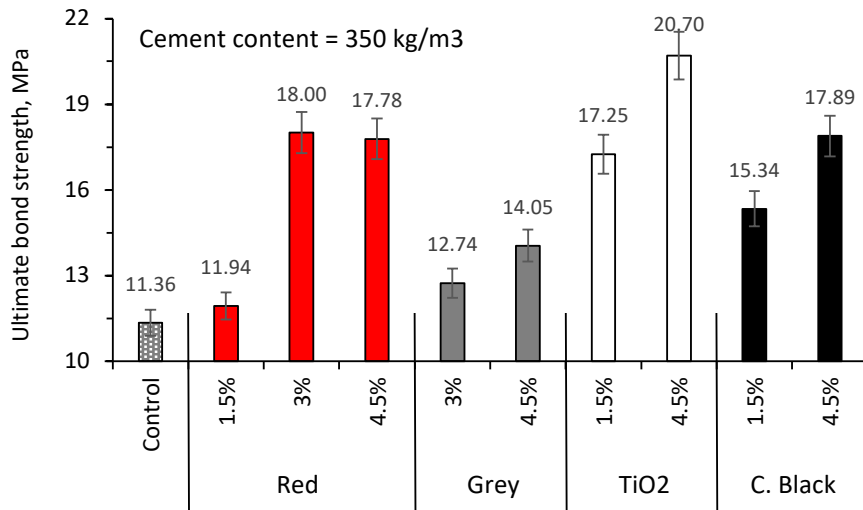


FIGURE 9. Effect of pigment type and concentration on τ_u for mixtures prepared with 350 kg/m³ cement.

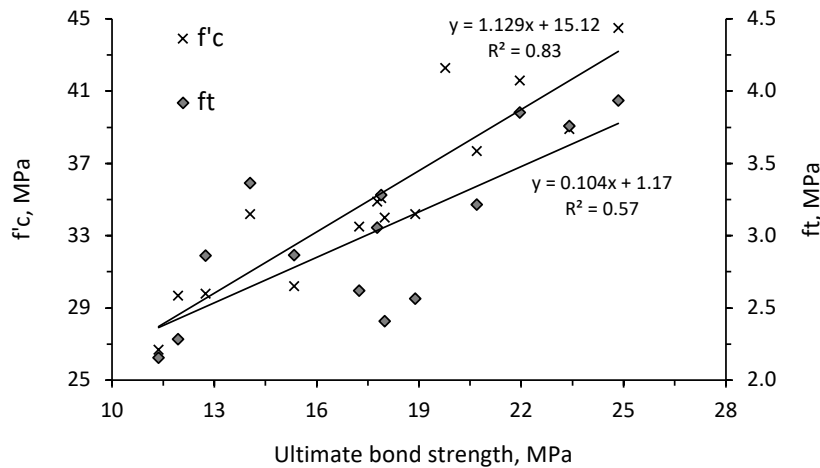


FIGURE 10. Relationships between τ_u with respect to $f'c$ and ft for all tested concrete mixtures.

embedded steel ribs and the surrounding concrete [32]. The 350-TiO₂-4.5% mixture exhibited the highest τ vs. δ responses, given the micro-filler effect and formation of secondary C-S-H hydrating compounds that strengthen the interfacial concrete-steel transition zone [26, 29]. Hence, compared to the 11.36 MPa value obtained from the control mix, τ_u reached 20.7 MPa for the 350-TiO₂-4.5% concrete. The increase in τ_u was also noticeable for mixtures prepared with IO pigments, albeit this remained comparatively lower than what was achieved with TiO₂ additions. Hence, τ_u reached 14.05 and 17.78 MPa for the 350-Grey-4.5% and 350-Red-4.5%, respectively. When the adhesive and interlock components fail, the concrete between the steel ribs breaks, causing excessive local slips at reduced bond stresses [42, 43]. Only the frictional bond component remains in the post-peak region of τ vs. δ curves, whereby the steel bars are dynamically pulled out from the concrete specimens.

Figure 9 summarizes the effect of the pigment type and concentration on τ_u responses determined for mixtures prepared with a 350 kg/m³ cement content.

Regardless of the pigment type, τ_u gradually increased with such additions, which practically reveals their beneficial role for improving the development and transfer of bond stresses in reinforced concrete members. The highest value of 20.7 MPa was recorded for the concrete containing the highest TiO₂ concentration of 4.5%. This was followed by mixtures incorporating 3% and 4.5% red IO as well as those made using 4.5% CB; the resulting τ_u hovered around 18 MPa. Just like the mechanical properties, the increase in τ_u due to inert IO or CB pigments can be attributed to the micro-filler effect that densifies the cementitious microstructure around the steel ribs, leading to an improved bond behaviour. Moderate relationships with R² of 0.57 and 0.83 are established between τ_u with respect to $f'c$ and ft for all tested concrete mixtures (Figure 10).

As shown in Figure 8, the increase in τ_u due to pigment additions is accompanied by an increase in the maximum slip that occurs at failure. For example, δ_u of 4.1 mm was registered for the 350-Control mix, while it reached 6.1 and 7.8 mm for the 350-Grey-

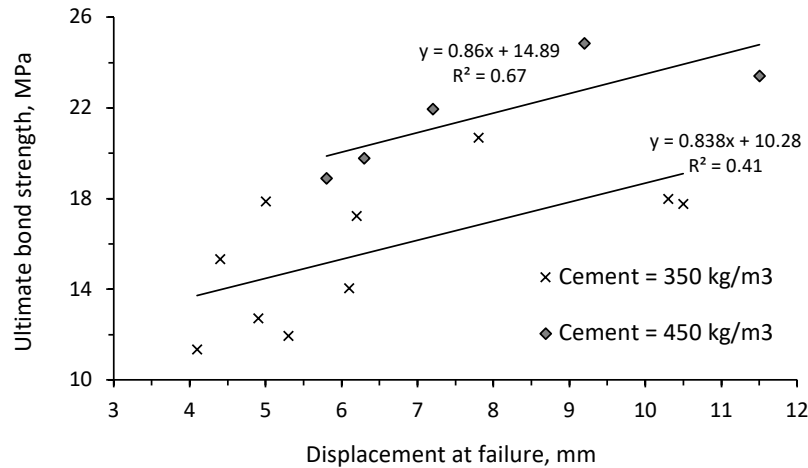


FIGURE 11. Relationships between τ_u and δ_u for mixtures prepared with 350 or 450 kg/m³ cement.

4.5% and 350-TiO₂-4.5%, respectively. In addition to the improved bond strength, this reflects that pigments confer higher ductility, which can be particularly relevant in high-strength concrete reinforced members [33, 43, 44]. Figure 11 plots the relationships between τ and δ for concrete mixtures prepared with 350 or 450 kg/m³ cement. Clearly, mixtures exhibiting higher τ_u are characterized by increased displacements at failure.

5. COMPARISON WITH INTERNATIONAL BOND MODELS

In order to ensure compliance of bond properties of the coloured concrete to international design code models, the τ_u values determined experimentally are compared with the design bond strengths (τ_{max}) specified in CEB-FIP [35], ACI 318-19 [33], and European Code EC2 [34] models. The CEB-FIP (2010) considers that the stiffness of ascending τ vs. δ curves follows an exponential trend raised to a power of 0.4, until reaching τ_{max} equal to 2 or 2.5 $\sqrt{f'_c}$, depending on whether the concrete is confined or not. This can be expressed in Eqs. 1 and 2 as follows.

CEB-FIP for unconfined concrete:

$$\tau_{max} = 2\sqrt{f'_c} \quad (1)$$

CEB-FIP for confined concrete:

$$\tau_{max} = 2.5\sqrt{f'_c} \quad (2)$$

In ultimate state conditions, the ACI 318-19 [33] considers that τ_{max} can be calculated as:

$$\tau_{max} = \frac{10\sqrt{f'_c} \left(\frac{C_b + K_{tr}}{d_b} \right)}{4 \times 9 \Psi_t \Psi_e \Psi_s \lambda} \quad (3)$$

where C_b is the concrete cover and K_{tr} the transverse reinforcement index (note that the $(C_b + K_{tr})/d_b$ ratio is limited to 2.5). The Ψ_s , Ψ_e , Ψ_t , and λ factors refer to the bar-size, epoxy coated bars, bar location with

respect to the upper surface, and lightweight concrete, respectively. In this study, Ψ_s is taken as 0.8 for bars No. 13, while Ψ_t , Ψ_e , and λ equal to 1.

The τ_{max} expression proposed by EC2 [34] for determining the ultimate bond stress is given as:

$$\tau_{max} = 2.25 \eta_1 \eta_2 f_{ctd} \quad (4)$$

where η_1 is a coefficient reflecting the bond quality to the embedded steel (taken as 1.0) and η_2 is related to the bar diameter (taken as 1, given that d_b is less than 32 mm). The $f_{ctd} = \alpha_{ct} f_{ctk,0.05}/\gamma_c$ refers to concrete design tensile strength, where α_{ct} and γ_c refer to the long-term effects on tensile strength and partial safety factor, respectively (both taken as 1). The $f_{ctk,0.05}$ refers to the concrete characteristic axial tensile strength computed as $0.7 \times 0.3 \times f_{ck}^{(2/3)}$, where f_{ck} is the 28-days compressive strength concrete cylinder.

Table 4 summarizes the τ_{max} values computed using the different codes as well as the resulting experimental-to-design bond strength ratios (i.e., τ_u/τ_{max}). As shown in Figure 12, the τ_{max} values followed an increasing trend with pigment additions. On average, the experimental τ_u values are 3.35- and 4.85-times higher than the ACI 318-19 and EC2 equations (Table 4), respectively; this reveals the conservative nature of such models for predicting the bond strength between steel bars and coloured concrete structures. Yet, the τ_u/τ_{max} becomes pretty close or even lower than 1.0 when the CEB-FIP equations are used (i.e., Eqs. 1 and 2), reflecting the unconservative nature of such equations for assessing the bond strengths of coloured concrete.

6. CONCLUSIONS

This paper is part of an investigation that aims at investigating the impact of pigments on the structural properties of reinforced coloured concrete members. The findings of this paper reveal that such additions have a rather beneficial effect on the concrete bond

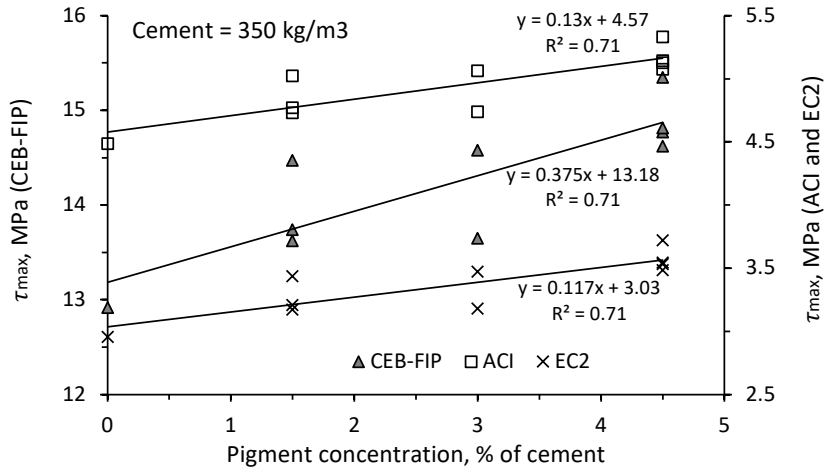


FIGURE 12. Relationships between pigment concentration and τ_{max} computed by different codes for mixtures prepared with 350 kg/m³ cement.

Mixture codification	τ_{max} computed by different codes				Experimental-to-design bond ratio				
	MPa				(τ_u/τ_{max})				
	$2\sqrt{f'_c}$	$2.5\sqrt{f'_c}$	ACI 318	EC2	$2\sqrt{f'_c}$	$2.5\sqrt{f'_c}$	ACI 318	EC2	
350-Control	10.3	12.9	4.5	3	1.1	0.88	2.53	3.84	
350-Red-1.5 %	10.9	13.6	4.7	3.2	1.1	0.88	2.52	3.76	
350-Red-3 %	11.7	14.6	5.1	3.5	1.54	1.23	3.56	5.19	
350-Red-4.5 %	11.8	14.8	5.1	3.5	1.5	1.2	3.47	5.03	
350-Grey-3 %	10.9	13.6	4.7	3.2	1.17	0.93	2.69	4.01	
350-Grey-4.5 %	11.7	14.6	5.1	3.5	1.2	0.96	2.77	4.03	
350-TiO ₂ -1.5 %	11.6	14.5	5	3.4	1.49	1.19	3.43	5.02	
350-TiO ₂ -4.5 %	12.3	15.4	5.3	3.7	1.69	1.35	3.88	5.57	
350-CBlack-1.5 %	11	13.7	4.8	3.2	1.4	1.12	3.22	4.78	
350-CBlack-4.5 %	11.8	14.8	5.1	3.5	1.51	1.21	3.48	5.04	
450-Control	11.7	14.6	5.1	3.5	1.62	1.29	3.72	5.42	
450-Red-3 %	12.5	15.6	5.4	3.8	1.88	1.5	4.32	6.16	
450-Grey-3 %	13	16.3	5.6	4	1.52	1.22	3.5	4.93	
450-TiO ₂ -3 %	13.3	16.7	5.8	4.2	1.86	1.49	4.29	5.98	
450-CBlack-3 %	12.9	16.1	5.6	4	1.7	1.36	3.92	5.53	
					Average =	1.45	1.16	3.35	4.85
					St. Deviation =	0.26	0.2	0.59	0.77

TABLE 4. Experimental-to-design bond strengths computed by different codes.

properties to embedded steel bars, which could practically be assuring to consultants and architects in the concrete building industry. Based on the foregoing, the following conclusions can be warranted:

- Mixtures containing TiO₂ exhibited the lowest $\Delta(E)$ values, reflecting relatively limited variations with respect to the control mix. The incorporation of gradually increased red or grey IO pigments led to an increased $\Delta(E)$, while the CB-modified mixtures exhibited the highest $\Delta(E)$ values.
- The steady $\Delta(E)$ increase with pigment additions was attributed to the relatively reduced cement volume and beige-like colour of natural sand, thus affecting the pigment tinting strength and reducing the tendency towards colour saturation.
- Regardless of the colour, mixtures incorporating increased pigment additions exhibited higher $f'c$ and ft responses. This was directly associated to the micro-filler effect and enhanced packing density that lead to denser microstructure. The IO and CB pigments are inert materials (i.e., do not react with water) that fill the interspaces and capillary pores in cementitious systems, leading to improved strength properties.
- The highest increase in strength was recorded for mixtures prepared with TiO₂ additions. Besides the micro-filler effect, the increase in strength was ascribed to the formation of nucleation sites that promote hydration reactions and reduce the porosity of the hardened matrix.
- Just like the $f'c$ and ft responses, τ_u gradually increased with such additions, which practically reveals their beneficial role for improving the development and transfer of bond stresses in reinforced concrete members. The highest increase was noticed for the concrete mixture containing TiO₂ additions, given the micro-filler effect and formation of additional hydrating gels that strengthen the interfacial concrete-steel transition zone.
- The increase in τ_u due to pigment additions was accompanied with an increase in the maximum slip that occurs at failure. This reflects that pigments confer higher ductility, which can be particularly relevant in high-strength concrete reinforced members.
- On average, the experimental τ_u values are 3.35- and 4.85-times higher than the ACI 318-19 and EC2 equations, respectively. Yet, the τ_u becomes pretty close to τ_{max} computed by the CEB-FIP equations, reflecting the unconservative nature of such equations to predict the bond strengths of coloured concrete mixtures.

ACKNOWLEDGEMENTS

The authors wish to acknowledge the support provided by Sodamco-Weber, Lebanon.

REFERENCES

- [1] P. Bartos. *Fresh concrete properties and test*. Elsevier, Amsterdam, 1992.
- [2] L. Popelová. The symbolic-aesthetic dimension of industrial architecture as a method of classification and evaluation: the example of bridge structures in the Czech republic. *Acta Polytechnica* **47**(1):23–31, 2007. <https://doi.org/10.14311/912>.
- [3] ASTM C979. Standard specification for pigments for integrally colored concrete. Annual book of ASTM standards. Farmington Hills, USA, 4(2), 2007.
- [4] V. Hospodarova, J. Junak, N. Stevulova. Color pigments in concrete and their properties. *Pollack Periodica* **10**(3):143–151, 2015. <https://doi.org/10.1556/606.2015.10.3.15>.
- [5] S. R. Naganna, H. A. Ibrahim, S. P. Yap, et al. Insights into the multifaceted applications of architectural concrete: A state-of-the-art review. *Arabian Journal for Science and Engineering* **46**:4213–4223, 2021. <https://doi.org/10.1007/s13369-020-05033-0>.
- [6] Y.-M. Gao, H.-S. Shim, R. H. Hurt, et al. Effects of carbon on air entrainment in fly ash concrete: The role of soot and carbon black. *Energy Fuels* **11**(2):457–462, 1997. <https://doi.org/10.1021/ef960113x>.
- [7] K. Loh, C. C. Gaylarde, M. A. Shirakawa. Photocatalytic activity of ZnO and TiO₂ ‘nanoparticles’ for use in cement mixes. *Construction and Building Materials* **167**:853–859, 2018. <https://doi.org/10.1016/j.conbuildmat.2018.02.103>.
- [8] S. S. Lucas, V. M. Ferreira, J. L. Barroso de Aguiar. Incorporation of titanium dioxide nanoparticles in mortars – Influence of microstructure in the hardened state properties and photocatalytic activity. *Cement and Concrete Research* **43**:112–120, 2013. <https://doi.org/10.1016/j.cemconres.2012.09.007>.
- [9] H.-S. Jang, H.-S. Kang, S.-Y. So. Color expression characteristics and physical properties of colored mortar using ground granulated blast furnace slag and White Portland cement. *KSCE Journal of Civil Engineering* **18**(4):1125–1132, 2014. <https://doi.org/10.1007/s12205-014-0452-z>.
- [10] R. Alves, P. Faria, A. Brás. *Brita Lavada – An eco-efficient decorative mortar from Madeira Island*. *Journal of Building Engineering* **24**:100756, 2019. <https://doi.org/10.1016/j.jobbe.2019.100756>.
- [11] J. J. Assaad, D. Nasr, S. Chwaifaty, T. Tawk. Parametric study on polymer-modified pigmented cementitious overlays for colored applications. *Journal of Building Engineering* **27**:101009, 2020. <https://doi.org/10.1016/j.jobbe.2019.101009>.
- [12] J. J. Assaad. Disposing waste latex paints in cement-based materials – effect on flow and rheological properties. *Journal of Building Engineering* **6**:75–85, 2016. <https://doi.org/10.1016/j.jobbe.2016.02.009>.
- [13] H.-S. Lee, J.-Y. Lee, M.-Y. Yu. Influence of inorganic pigments on the fluidity of cement mortars. *Cement and Concrete Research* **35**(4):703–710, 2005. <https://doi.org/10.1016/j.cemconres.2004.06.010>.

- [14] A. Woods, J. Y. Lee, L. J. Struble. Effect of material parameters on color of cementitious pastes. *Journal of ASTM International* **4**(8):1–18, 2007. <https://doi.org/10.1520/JAI100783>.
- [15] T. Meng, Y. Yu, X. Qian, et al. Effect of nano-TiO₂ on the mechanical properties of cement mortar. *Construction and Building Materials* **29**:241–245, 2012. <https://doi.org/10.1016/j.conbuildmat.2011.10.047>.
- [16] A. Mohammed, N. T. K. Al-Saadi, J. Sanjayan. Inclusion of graphene oxide in cementitious composites: state-of-the-art review. *Australian Journal of Civil Engineering* **16**(2):81–95, 2018. <https://doi.org/10.1080/14488353.2018.1450699>.
- [17] A. López, J. M. Tobes, G. Giaccio, R. Zerbino. Advantages of mortar-based design for coloured self-compacting concrete. *Cement and Concrete Composites* **31**(10):754–761, 2009. <https://doi.org/10.1016/j.cemconcomp.2009.07.005>.
- [18] L. Hatami, M. Jamshidi. Application of SBR-included pre-milled colored paste as a new approach for coloring self-consolidating mortars (SCMs). *Cement and Concrete Composites* **65**:110–117, 2016. <https://doi.org/10.1016/j.cemconcomp.2015.10.015>.
- [19] P. Weber, E. Imhof, B. Olhaut. Coloring pigments in concrete: Remedies for fluctuations in raw materials and concrete recipes. Tech. Report, Harold Scholz & Co GmbH, 2009.
- [20] J. J. Assaad, M. Vachon. Valorizing the use of recycled fine aggregates in masonry cement production. *Construction and Building Materials* **310**:125263, 2021. <https://doi.org/10.1016/j.conbuildmat.2021.125263>.
- [21] M. J. Positieri, P. Helene. Physicomechanical properties and durability of structural colored concrete. In *ACI Symposium Publication*, vol. 253, pp. 183–200. 2013. <https://doi.org/10.14359/20175>.
- [22] S. A. Yildizel, G. Kaplan, A. U. Öztürk. Cost optimization of mortars containing different pigments and their freeze-thaw resistance properties. *Advances in Materials Science and Engineering* **2016**:5346213, 2016. <https://doi.org/10.1155/2016/5346213>.
- [23] S. Masadeh. The effect of added carbon black to concrete mix on corrosion of steel in concrete. *Journal of Minerals and Materials Characterization and Engineering* **3**(4):271–276, 2015. <https://doi.org/10.4236/jmmce.2015.34029>.
- [24] D. Inoue, H. Sakurai, M. Wake, T. Ikeshima. Carbon black for coloring cement and method for coloring molded cement article. European patent, WO 01/046322, 10 p, 1999.
- [25] J. Topič, Z. Prošek, K. Indrová, et al. Effect of pva modification on properties of cement composites. *Acta Polytechnica* **55**(1):64–75, 2015. <https://doi.org/10.14311/AP.2015.55.0064>.
- [26] A. Nazari, S. Riahi. The effect of TiO₂ nanoparticles on water permeability and thermal and mechanical properties of high strength self-compacting concrete. *Materials Science and Engineering: A* **528**(2):756–763, 2010. <https://doi.org/10.1016/j.msea.2010.09.074>.
- [27] J. Chen, S.-C. Kou, C.-S. Poon. Hydration and properties of nano-TiO₂ blended cement composites. *Cement and Concrete Composites* **34**(5):642–649, 2012. <https://doi.org/10.1016/j.cemconcomp.2012.02.009>.
- [28] R. Zhang, X. Cheng, P. Hou, Z. Ye. Influences of nano-TiO₂ on the properties of cement-based materials: Hydration and drying shrinkage. *Construction and Building Materials* **81**:35–41, 2015. <https://doi.org/10.1016/j.conbuildmat.2015.02.003>.
- [29] A. Folli, C. Pade, T. B. Hansen, et al. TiO₂ photocatalysis in cementitious systems: Insights into self-cleaning and depollution chemistry. *Cement and Concrete Research* **42**(3):539–548, 2012. <https://doi.org/10.1016/j.cemconres.2011.12.001>.
- [30] M. Konrad, R. Chudoba. The influence of disorder in multifilament yarns on the bond performance in textile reinforced concrete. *Acta Polytechnica* **44**(5-6):186–193, 2004. <https://doi.org/10.14311/654>.
- [31] J. J. Assaad, P. Matar, A. Gergess. Effect of quality of recycled aggregates on bond strength between concrete and embedded steel reinforcement. *Journal of Sustainable Cement-Based Materials* **9**(2):94–111, 2020. <https://doi.org/10.1080/21650373.2019.1692315>.
- [32] ACI 408R-03. Bond and development of straight reinforcing bars in tension, 2003.
- [33] ACI 318-19. Building code requirements for reinforced concrete, 2019.
- [34] EN 1992-1-1. Eurocode 2: design of concrete structures – part 1-1: general rules and rules for buildings, 2004.
- [35] FIB (International Federation for Structural Concrete). *Model Code for Concrete Structures*. Ernst & Sohn, Berlin, 2013.
- [36] ASTM C642-13. Standard test method for density, absorption, and voids in hardened concrete. Annual book of ASTM standards. West Conshohocken, PA, 2013, USA.
- [37] ASTM C39/C39 M-05. Standard test method for compressive strength of cylindrical concrete specimens. Annual book of ASTM standards. West Conshohocken, PA, 2005, USA.
- [38] ASTM C496/C496 M-04. Standard test method for splitting tensile strength of cylindrical concrete specimens. Annual book of ASTM standards. West Conshohocken, PA, 2004, USA.
- [39] ASTM C 597-16. Standard test method for pulse velocity through concrete. Annual book of ASTM standards. West Conshohocken, PA, 2016, USA.
- [40] G. Teichmann. The use of colorimetric methods in the concrete industry. *Betonwerk Fertigteil-Technik* **11**:58–73, 1990.
- [41] RILEM/CEB/FIB. Bond test for reinforcing steel: 2, pullout test. *Materials and Structures* **3**:175–178, 1970.
- [42] J. Němeček, P. Padevět, Z. Bittnar. Effect of stirrups on behavior of normal and high strength concrete columns. *Acta Polytechnica* **44**(5-6):158–164, 2004. <https://doi.org/10.14311/648>.

- [43] A. AlArab, B. Hamad, J. J. Assaad. Strength and durability of concrete containing ceramic waste powder and blast furnace slag. *Journal of Materials in Civil Engineering* **34**(1):04021392, 2022. [https://doi.org/10.1061/\(ASCE\)MT.1943-5533.0004031](https://doi.org/10.1061/(ASCE)MT.1943-5533.0004031).
- [44] J. Machovec, P. Reiterman. Influence of aggressive environment on the tensile properties of textile reinforced concrete. *Acta Polytechnica* **58**(4):245–252, 2018. <https://doi.org/10.14311/AP.2018.58.0245>.